A WIRELESS SENSOR FOR TOOL TEMPERATURE MEASUREMENT AND ITS INTEGRATION WITHIN A MANUFACTURING SYSTEM

Paul K. Wright, David A. Dornfeld, Robert G. Hillaire, and Nathan K. Ota.
The Berkeley Manufacturing Institute
University of California at Berkeley
Berkeley, CA 94720-1740

ABSTRACT

This is a systems-oriented paper that begins with a specific description of a wireless sensor that was developed to measure cutting tool temperatures in milling. Resistive Temperature Detectors (RTDs) were installed on the backside of end-mill inserts and a wireless platform transmitted data. The goal of this new work was to design a wireless sensor system with a high degree of miniaturization, together with the ability to measure temperatures in real-time. As a result, the new system could be used within an Open Architecture Controller (OAC) as part of a closed loop monitoring system based on a desired "operating set-point temperature." The second part of the paper describes a broader use of wireless sensors that can be integrated into factory-wide Wireless Sensor Networks (WSNs). Such networks are an underlying technology that can further broaden the effectiveness of Computer Integrated Manufacturing (CIM) Systems. The final section of the paper reviews the present standards, deployment strategies, and specific wireless platforms (including hardware examples and "TinyOS" operating systems) that needed to accelerate the use of WSNs in CIM.

INTRODUCTION

This paper builds upon last year's NAMRC publication by Merchant and the authors [1]. It described how modern global enterprises are unfolding into human-centered "Holonic Manufacturing Systems (HMSs)." Our ongoing research on HMSs aims to demonstrate concrete examples and applications. Specifically, we have focused on the use of Wireless Sensor Networks (WSNs) to monitor machinery, machine tools, and other production facilities; including energy monitoring in aluminum smelters [2]. WSNs introduce new capabilities for sensing, that are otherwise difficult to obtain with "wired" sensors. The ability to add wireless sensor platforms to any part of a machine, to re-orient them as needed, and then to have them "self-organize" into a mesh-network is a powerful capability. The small "mote" platforms described later – identical in their base performance but perhaps carrying different sensors – are indeed an example of holons as described by Koestler in 1954 (see [3]) and adopted by Merchant in his first descriptions of Holonic Manufacturing Systems (HMSs). Merchant's definition of an HMS means that all entities (people, machines, software elements, etc.) are technically enabled to communicate and cooperate globally.

MANUFACTURING SYSTEM INTEGRATION & REVIEW OF OTHER WORK

Figure 1 shows an Open Architecture Controller (OAC) that integrated the wireless sensor platform in Figure 2 and 3 for tool temperature measurement. The OAC used for this work was the third generation controller first developed in 1989 [4-6]. Open architecture controllers have matured over the last several years to include several commercially available components. Several other prominent efforts helped develop the modern open architecture controller [7-14].

Figure 1 is comprised of a DSP motion control card, a user interface, and a published set of APIs (that allowed access to the functional code on the DSP motion control card). These components were purchased from the Delta Tau Company. The Delta Tau Controller has three interface abstraction layers. The top layer is a customizable user interface (including manual machine inputs), which parses commands to the interpretation layer. The command parser can be customized if the established communication protocols are not violated. The interpretation (middle) layer handles the communication between the user interface and the lowest layer that operates in real-time. The interpretation layer may be modified to communicate with outside programs, if it maintains the existing communication structure between the user interface and real-time layers. The real-time layer handles the motor servo con-

trols, fine path interpolation, and real time digital inputs and outputs. This layer may be modified to create new servo algorithms, new digital IO interfaces, or fine interpolation methods [*see* Hillaire 2001]. The sensors mounted on the open architecture controller included: a Load Controls™ motor power monitor; a Kistler™ acoustic sensor; a Kistler™ vibration sensor; a Kistler™ 9281B table mounted dynamometer (force sensor); and the wireless temperature sensor.

EXPERIMENTAL TEMPERATURE METHOD

Overview

The general approach used was to measure the average temperature on the backside of the inserts and then to correlate that data with the rake face temperature (described in the later sections of the paper). The milling cutter used (Figure 3) was a ~31mm (1.25 inch) end-diameter indexable end-mill with two carbide inserts. The upper shank of the end-mill was 25mm in diameter. This was the smallest shank-diameter that was feasible for incorporation of the wireless sensor and commercial off-the-shelf indexable inserts (TPG322 C5 grade, uncoated). The tool holder shank geometry and its inserts were selected to create a zero-degree rake angle and zero-degree helix in order to simplify the on-line calculations.

In addition, again to simplify the on-line calculations, these standard inserts were custom ground to have a restricted contact length. Figure 4 shows the grooves that were created by the custom grinding, hence leaving a chip-tool contact length of 0.5mm. The calculations (see later) can thus conveniently assume conditions of full-seizure over the entire chip-tool contact length of 0.5mm (see Trent and Wright [15]). This contact length of 0.5mm is not the set length but the maximum length, since it will be seen (in the experimental section that the uncut chip thickness is smaller than the land value even at its highest value. Other insert data are as follows: Relief, 11 degrees; Tolerance, +/- 0.025mm; IC, 9.525mm; Thickness, 3.175mm; Corner radius, 0.794mm (Figure 4).

Measurement of Temperature

The temperatures were directly measured on the backside of the rotating tool's inserts, and then wirelessly transmitted to the computer controller for use in the closed control loop. Since the tool shank was only 25mm in diameter, the sensor package's PCB was designed to be a ~19mm disc-shaped platform that would neatly fit into the end of the standard size of the tool-shank. Surface mount technology was used to miniaturize the transmitter circuit as seen on the top of Figure

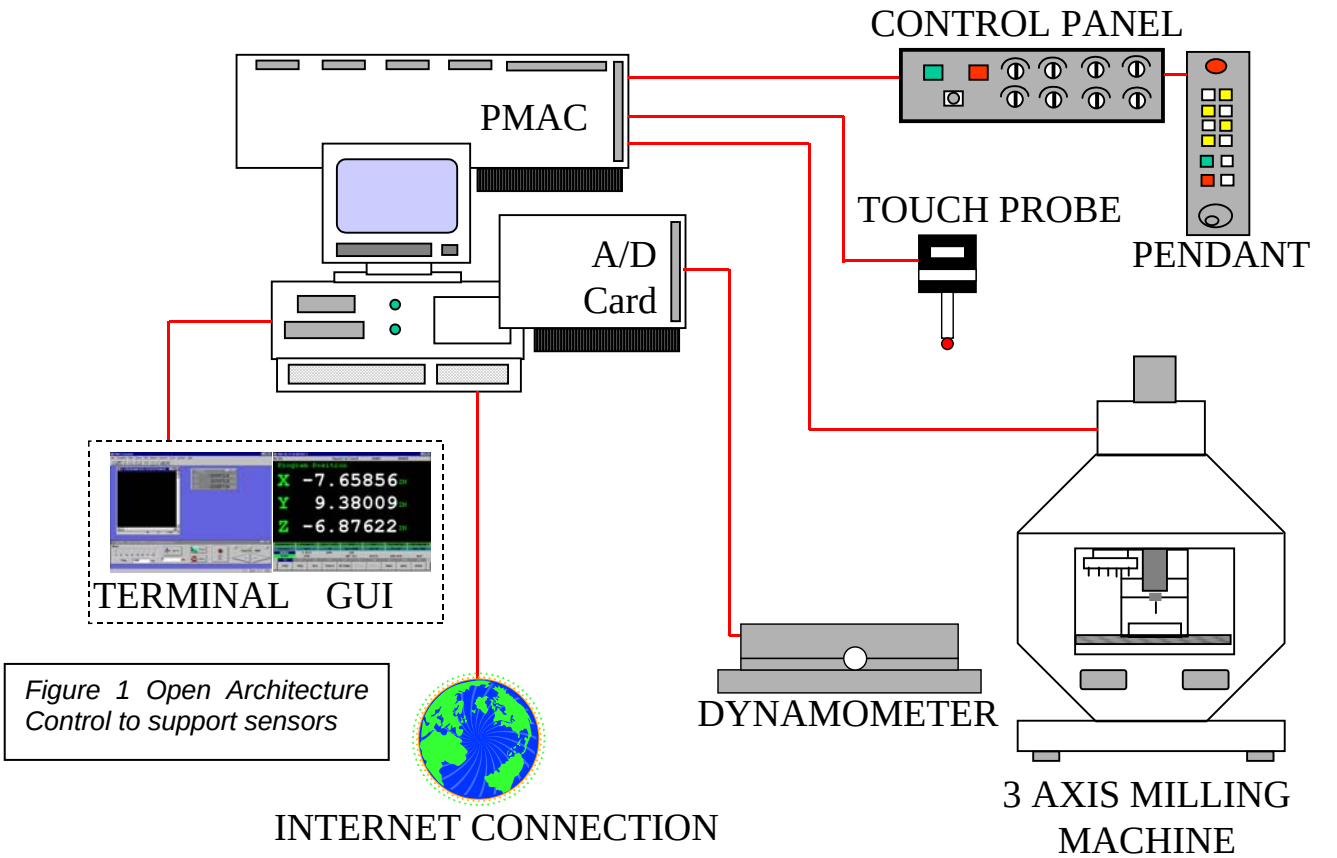

Figure 1 Open Architecture Control to support sensors

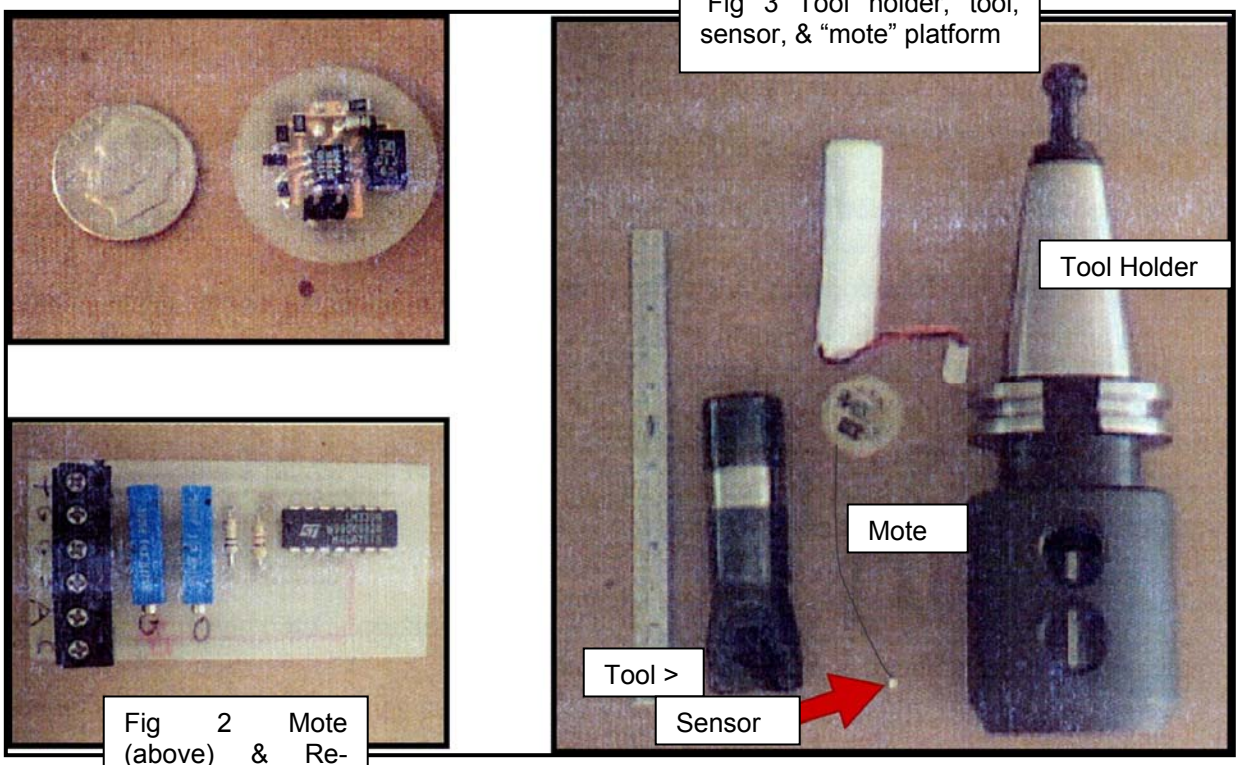

Fig 3 Tool holder, tool, sensor, & "mote" platform

Fig 2 Mote (above) & Receiver (below)

2. The decoding circuit that was used to amplify and square the received signal is shown on the bottom – this was mounted a short distance away from the rotating tool-spindle, close to the controller. The disc-shaped wireless sensor platform was connected with a thin wire to two Resistive Temperature Detectors (RTDs), one per insert backside [16]. The red arrow in Figure 3 shows the small white square that is one of the RTDs. The figure also shows the thin wire connecting the RTD to the disc-shaped wireless transmitter. The photograph also contains the white battery pack, the two-insert cutting tool on the left, and the larger tool-mandrel on the right. The RTDs were used because of their superior linearity with temperature value. (While thermocouples could also have been used, the RTD signals were directly proportional to temperature and hence easy transmit without complex signal processing). The RTD was one leg of a half bridge voltage divider. The custom circuit was composed of surface mount analog ICs that precisely generated a frequency proportional to a reference current through the RTD. The circuit generated a square wave frequency at about 50mA and 6V. This square wave drove the inductive antenna, which was made from 100 coils of magnet wire wrapped around the neck of the tool holder. The receiver isolated the peak, amplified and then squared the signal before sending to the frequency counter for temperature decoding.

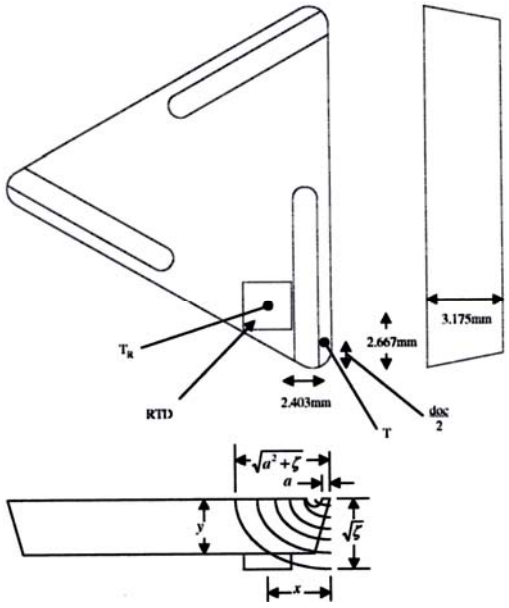

Figure 4 Tool Geometry

Wireless Transmission of RTD Temperature

The direct measurement of temperature from an insert in a spinning milling cutter was perhaps the most challenging aspect of this work. The small

Resistive Temperature Detector (RTD) was glued to the back of the insert at the position shown in the very bottom of Figure 4. The thin wire above the arrow in Figure 3 connected the RTDs to the disc-shaped transmitter platform that was fitted into the far end of the shank.

The circuit on the disc (Figure 2a) was designed and prototyped to create a frequency output that varied according to a resistive change on the RTD. The frequency of this circuit was passed through an amplifier to an inductive emitter. An inductive antenna collected the magnetic field produced by the emitter. This signal was amplified and filtered to produce a square wave that could be counted on a data acquisition card. The frequency of the RTD circuit is given by f = V/10RC. Here, V is the voltage across the RTD leg of the half bridge circuit. Hillaire [16] describes the detailed calibration procedures using a series of calibrated baths and furnaces. The relationship was sufficiently linear over the operating range as shown in Figure 5. The pulses generated by the circuitry were counted for one tenth of a second per sample. This provided a 10Hz resolution (corresponding to ~0.7 degrees).

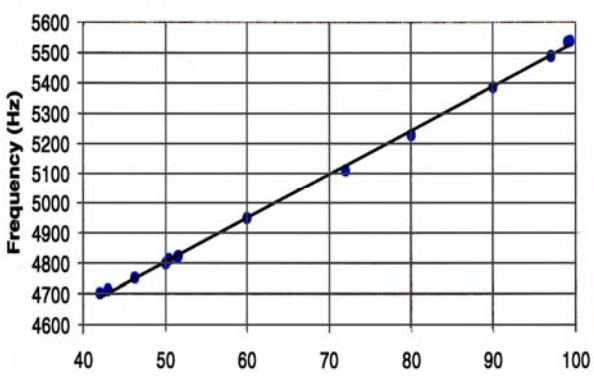

Figure 5: Calibration over the main operating range of the backside RTD sensor

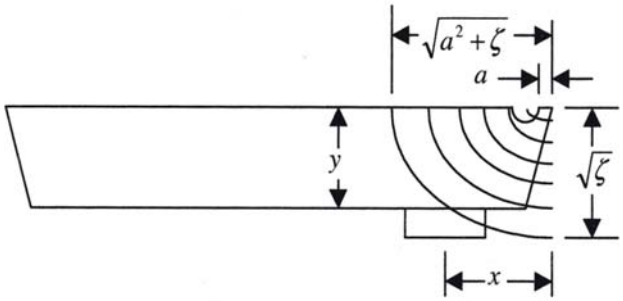

Figure 6: Typical temperature profiles

TEMPERATURE CALCULATION METHOD

Temperature Profiles and Contact Area

Previous work by Wright *et al* [17, 18] showed that the average *surface* temperature of the rake face may be directly correlated with the insert's *backside* temperature using the profiles of the temperature isotherms shown in Figure 6 through 8. The correlation is first based on the many experimentally obtained examples of heat distribution shown by Trent and Wright [15]. When machining continuous chip materials such as most steel and aluminum alloys, the isotherms radiate as elliptical shells from the contact area on the rake face as shown in Figure 6.

Pre-grinding to create the controlled area of contact (Figure 4 and 6) defines the heat source and consequent isotherms with more repeatability. At high cutting speeds typical of commercial operations, this contact area may be assumed to be full-seizure conditions so that the heat source is proportional to the shear strength of the workmaterial in the secondary shear zone.

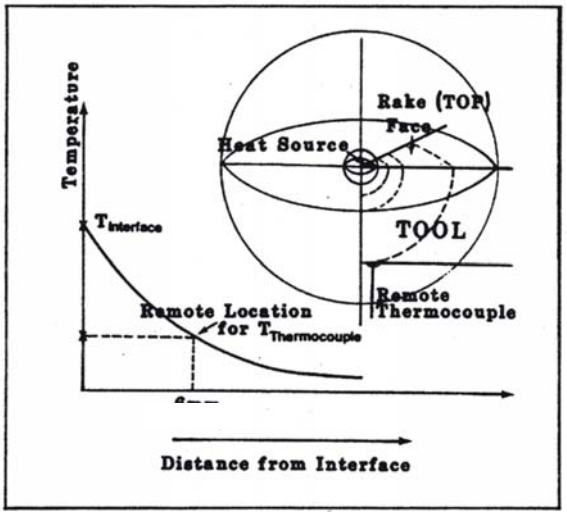

Figure 7: Elliptical profile and relation between backside RTD and rake face elliptical heat source

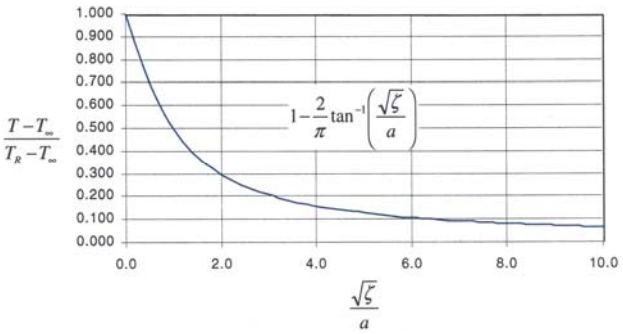

Figure 8: Temperature profile through thickness of tool (rake face on left vertical axis)

Relation between Rake Face and RTD position

Wright *et al* [17, 18] modeled the profile through the tool as an ellipse. This led to the graph above in Figure 8 and the following equation to estimate the rake face temperature from the remote temperature, measured in this work by the RTD and wireless transmission:

$$\frac{T-T_\infty}{T_R-T_\infty} = 1-\frac{2}{\pi}\tan^{-1}\left(\frac{\sqrt{\zeta}}{a}\right)$$

In the above equation, the temperature T of the tool rake face is expressed in terms of the remote temperature reading T_R and room temperature T_∞ by the length of the controlled chip-tool contact area, a, and the distance away from the rake face measured in terms of $\sqrt{\zeta}/a$. (Note that the insert was 3.175mm thick but that the above graph is plotted non-dimensionally).

EXPERIMENTAL RESULTS

Rake Face Temperatures

A variety of steel workmaterials were chosen to test the system: a 12L14 free machining steel, AISI 1020, and AISI 1045 steel. Some of the results from [16] are tabulated in Table 1 with measured temperatures of the controlled-contact land. It must be pointed out these results are for full-slot end-milling, and that "aggressive" machining conditions were chosen in order to stimulate high temperatures that could easily be measured by the overall system. As might be expected the free-machining steel 12L14 showed the lowest temperatures of the 3 test samples. The higher carbon content and consequent hardness of AISI 1045, in comparison with 1020, was also evident in the results. Again as expected temperatures rose with increasing cutting speed for a fixed feed rate. Further experiments are planned with more workmaterials and conditions. Before discussing control we re-emphasize that the above results are at relatively high cutting speeds chosen to create high, easily measured temperatures. They are higher than the normal cutting speeds that would be chosen to give an economic tool life.

Material	**Speed**	**Feed**	**$T_{thiswork}$**
AISIspec.	*m/min*	*mm*	*^oC*
12L14	75	0.178	725
12L14	105	0.178	741
12L14 (*)	125	0.178	768
AISI1020	75	0.178	1055
AISI1020	90	0.178	1153
AISI1020	105	0.178	1254
AISI1045	75	0.178	1207
AISI1045	90	0.178	1213
AISI1045	105	0.178	1218

Table 1: Rake face temperatures for 3 steels during full-slot end-milling. (*) Higher speeds were possible with 12L14, whereas 1020 and 1045 were more or less at their limit at 105m/min.

Set-point for Control

Consequently, in terms of using the tables above for Open Architecture Control, it was important to view the values in Table 1 as the "top-speed/highest-temperature" operating conditions. For longer life in the experiments, the cutting speeds – and hence temperatures – were reduced to values that were below the hot compressive strength of the inserts thus avoiding plastic deformation of the tool in the controlled-contact area and with it, the collapse of the vulnerable cutting edge. For example, Figure 9 shows Trent and Wright's hot compressive strength results of four tool materials with the best comparison to the TPG322 C5 grade, uncoated inserts being the (WC+12%TiC+7%cobalt) shown last on the right. Here, it can be seen that below ~1,080^{o}C the (WC+12%TiC+7%cobalt) will not fail by plastic collapse. Hence, for control, this value was used for the "set point" for the rake face area just back from the edge. In this way, cutting conditions were viewed as "safe but productive."

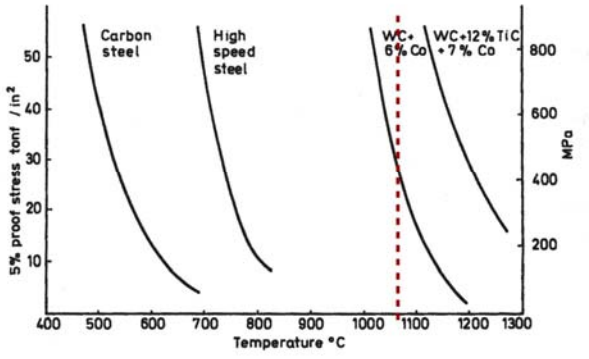

Figure 9: Hot compression tests: proof stress of tool steels and cemented carbide, used to determine the "set-point" for "safe-but-productive" cutting (vertical dashed line). (WC+12%TiC+7%cobalt, shown at right.)

TECHNOLOGY DIRECTIONS

Generic Hardware Platforms for Sensors

The wireless platform in Figure 2 was developed in an *ad hoc* manner in the year 1999 for the specific support of the RTD temperature sensor [16]. Based on its promising ability to provide sensor readings in a rotating and usually inaccessible location, further work began on measuring localized forces and vibrations. However, rather than also proceed in an *ad hoc* fashion for these sensors it was apparent, at that time, that a new family of devices called "motes" (so named for their miniature size) was becoming available in the market place [see www.xbow.com]: and that such "motes" could be a generic support platform for the creation of Wireless Sensor Networks (WSNs). These platforms continue to be refined and miniaturized by an increasing number of commercial ventures [see www.dust-networks.com] Figure 10 shows the evolution of such wireless sensor platforms: self-contained units that include the desired sensor(s), a small computer, a transmitter, and battery. Today's units, being used below, are 2 to 6cm^3 (Figure 10b and 10c). The platforms use commercial-off-the-shelf (COTS) radios to give a reliable range of 10ft., and a limit of 50ft. The next platforms will exploit highly integrated CMOS-radios to integrate analog and digital radio functions at low power consumption [19]. To achieve the desired flexibility of a mesh-network, an energy efficient operating system has been developed which allows the sensor platforms to communicate for several weeks on batteries. The Mica-02 platform (Figure 10b), from the DARPA "NEST" project, uses a simple 50Kb data-rate radio, and is supported by TinyOS [20]. TinyOS, written in C, has small physical size and low power consumption. It exhibits concurrency-intensive operations to support floods of sensor-data with multiple flows, providing a collection of state machines allowing control of a mesh-network.

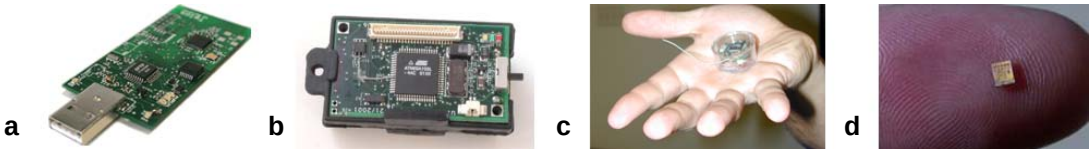

Figure 10a to 10d: Evolution of wireless sensor nodes of "motes". 10d shows a preliminary MEMS proof of concept.

Integration: Holonic Manufacturing Systems

At a conceptual level, a Wireless Sensor Network (WSN) comprises a set of devices or nodes that are organized in the form of a network. Each node has a microcontroller to perform basic computations, memory to store executable code and data, and a radio to enable bi-directional communication. A variety of sensors can be integrated into and controlled by the node. As a result the nodes in a WSN do indeed fulfill the definition of a holon, [3], and as described by Merchant, can be the low-level building blocks for Holonic Manufacturing Systems (HMS). The sensor platforms (or "motes") shown here can also be readily incorporated into the operations of Open Architecture Controllers that comprise the important, mid-level building blocks of such HMSs.

Performance, Energy, and Reliability

This new class of communication infrastructure is uniquely constrained by the energy consumption of nodes and the reliability of the ultra-low power radios. Traditional constraints such as latency and throughput remain important as well. Each constraint is related to the other as discussed below.

Energy is commonly referred to as the main constraint for wireless sensor network applications. This assumes a minimum lifetime objective for a node that has a finite energy source and/or power source. This also assumes line-power or unconstrained battery capacity are not viable options. Energy estimates can be expressed as the summation of the energy expended for sensing, computing, and transmitting data, as well as maintaining state in a low-power mode often referred to as sleeping. Typically, the wireless sensor node, as shown in Figure 10, consumes microwatts of power sleeping, single digit milliwatts sensing and computing, and tens of milliwatts communicating. Sensing and computation often require much less time, and therefore energy, than transmitting or receiving. Maximizing sleeping time minimizes energy consumption and maximizes life of the node and network. Manufacturing applications, however, potentially pose two energy constraints through power and time. First, sensors designed for line-powered implementations may require hundreds of milliwatts of power over several seconds. An example is vibration sensors for vibra-

tion analysis. Even at low sampling frequencies, a modestly sized battery would quickly exhaust its energy reserves. Conversely, applications may require a relatively high sampling frequency, precluding approaches to maximize node life by extensive sleeping. The RTD application described previously exemplifies this scenario. At 10 Hz sampling frequency, an ample battery will only last approximately 3000 hours. Parameters are as follows: Battery capacity, 600mAH; Transmission power 60mW; Bit rate, 250 kbps; Packet size, 36 bytes; Sleep power, 0 mW; Sense/Computation power, 0 mW.

Reliability is a constraint at the node as well as the network since radio communication is inherently lossy. While traditional approaches are still valid in addressing physical failures, failure is also equivalent to a node exhausting the energy supply. Individual node failures can have ripple effects for network reliability since mesh networking inherently relies on all nodes to achieve reliable communication. Constraints on mean time between failures not only pertain to the node, but also how the network reacts to failed nodes. As well, ultra-low power radio communication is particularly susceptible to bit corruption in heavy electromagnetic field environments that often exist in manufacturing facilities. Unlike known wired links, wireless communication links are also susceptible to a host of wireless-specific problems such as hidden nodes that affect communication.

Lastly, *latency* and *throughput* constraints posed by wireless sensor networks spur from the substitution of low-power radios for wired communication links as the physical medium for communication. By definition, wireless sensor networks are defined by low data rates with typical radio transmission rates, and typically range from 10 kbps to 250 kbps. Seemingly greater than typical sensor networking technologies like HART (1.2 kbps) or Foundation Fieldbus (31.25 kbps), available bandwidth decreases with the number of nodes, as with any shared medium. For example, a ten node network of 250 kbps radios would have a maximum throughput of 25 kbps per node assuming a simple time division media access control scheme using narrow band radio communication.
Methods to improve latency and throughput with in-situ data aggregation and processing are well explored; however, these methods inherently require energy tradeoffs as well.

In summary, these new technology directions in wireless sensing and networking influence CIM at a variety of levels. *First*, at the lowest level of actual sensing, there is the obvious replacement of wires for sensing opportunities in previously inaccessible locations (as achieved by Figure 3.) *Second*, at the next level concerning data analysis, as the platforms in Figure 10 become more capable of on-board analysis they will work with machine controllers (*see* Figure 1) for more effective closed loop control. (It must be admitted, however, that energy consumed, reliability, latency, and throughput constraints of today's devices are considerations that require redundant nodes to be set up in networks in order to ensure overall reliability.) *Third*, to support the engineering staff at the enterprise level, this detailed understanding of the behavior of individual machines such as Figure 1 – also extended to the many other machines within a Computer Integrated Manufacturing (CIM) – will create more information and knowledge for planning and scheduling, thus enabling distributed control.

CONCLUSION

1. A wireless system was developed for cutting tool temperature measurement. The system was designed for miniaturization in order to fit into a standard indexable end-mill system (Figure 3).

2. Temperatures were measured on the backside of the indexable inserts during full-slot end-milling. Resistive Temperature Detectors (RTDs) – one of which is arrowed in Figure 3 – were the key sensor devices. Within the tool-shank itself, RTDs were connected to small internal platforms that could then transmit the temperature data to a nearby receiver for data acquisition and analysis.

3. A previous analysis by Wright *et al* [17,18] was used to calculate the rake face temperature from the backside temperature.

4. Results were obtained for 3 workmaterials: a 12L14 free machining steel; AISI 1020; and AISI 1045 plain carbon steels. Temperatures, as expected, increased with speed for a given feed and with the carbon content of the workmaterials.

5. The wireless temperature system was integrated into the Open Architecture Controller (OAC) built in previous work [16]. The closed loop control of the OAC was employed to run the milling operation at a desired "temperature-set-point."

6. This temperature-set-point was determined from Trent and Wright's [15] data on the hot compressive, 5% proof stress of the cemented carbide (WC+12%TiC+7%cobalt). This value determined a "set-point" for "safe-but-productive" cutting (the vertical dashed line shown in Figure 9).

7. The platforms in Figure 10a-c can carry a supplementary sensor board for a variety of sensors -- hence providing new opportunities to re-visit much previous work in sensor based machining, that was perhaps limited by "wired" connections and hence less accessibility [21]. Further work is thus planned to investigate coolants, tool wear, dynamic conditions and other OAC strategies.

ACKNOWLEDGMENT
The equipment in Figure 1 was funded by the National Science Foundation's DMII division under various grants. Any opinions, findings, and conclusions or recommendations expressed in this material are those of the authors and do not necessarily reflect the views of NSF

REFERENCES

1. M.E. Merchant, D.A. Dornfeld and P.K. Wright, "Manufacturing: It's Evolution and Future," Transactions of the North American Manufacturing Research Institution, 2005, Volume 33, pp. 211-218.

2. M. H. Schneider, J. W. Evans, P. Wright, D. Ziegler and D. Steingart, "Experiments on Wireless Instrumentation of Hall Cells", Light Metals 2005 pp. 407-412.

3. A. Koestler. The Ghost in the Machine. Arkana Books, 1989.

4. Greenfeld, I., Hansen, F., Fehlinger, J., and Pavlakos, E., "MOSAIC System Description, Specification and Planning," Technical Report No. 452, Robotics Report No. 201, NYU, Courant Institute of Mathematical Sciences. 1989.

5. Schofield, S.M., "Open architecture controllers for advanced machine tools," University of California, Berkeley Doctoral Dissertation, 1995.

6. Marchetti, L., "MOSAIC-PC: A Multimedia Manufacturing Testbed" University of California, ESRC Report "ESRC 97-15" December, 1997

7. Altintas, Y., "A Hierarchical Open-Architecture CNC System for Machine Tools," Annals of the CIRP, Vol. 43, 1994, pp. 349-354.

8. Altintas, Y., Newell, N., and Ito, M., "Modular CNC design for intelligent machining, Part 1: Design of a hierarchical motion control module for CNC machine tools," J. of Manufacturing Science and Engineering, 1996; v.118, no.4, p.506-513

9. Kasashime, N., Mori, K., and Yamane, T., "An Intelligent Numerical Controller for Machining System," Modern Tools for Manufacturing Systems, 1993, pp. 77-85.

10. Lo, C. and Koren, Y., "Evaluation of Servo-Controllers for Machine Tools" 1992 American Control Conference Vol. 1., 1992, pp 370-374.

11. Orban, P., Yellowley, I., and Zhou, Y., "Open Architecture Controllers: Development Platform for Machine Tool Control Applications" American Society of Precision Engineers Conference, 1994

12. Proctor, F. and Michaloski, J., "Enhanced machine controller: Architecture Overview," Manufacturing Engineering Laboratory, NIST, 1994.

13. Teltz, R. and Elbestawi, M.A., "On the Design of an Open Architecture Controller for Machine Tool Systems" Intelligent Automation and Soft Computing, TSI Press, 1994, pp. 237-243.

14. Yellowley, I. and Pottier, P.R., "The Integration of Process and Geometry within an Open Architecture Machine Tool Controller," International Journal of Machine Tools and Manufacture, Vol. 34 No. 2, 1994, pp. 277-293.

15. Trent, E.M., and Wright, P.K. *Metal Cutting, 4th Edition*, Butterworth Heinemann, Newton MA, published in January 2000.

16. Hillaire, R.G., "New Machining Strategies with Open Architecture Controllers," University of California, Berkeley Doctoral Dissertation, 2001.

17. P.K. Wright, "Physical Models of Tool Wear for Adaptive Control in Flexible Machining Cells," CIM/PED- 8, ASME, 1984, pp. 19-31.

18. D.W. Yen and P.K. Wright, "Adaptive Control in Machining: A New Approach Based on the Physical Constraints of Tool Wear Mechanisms," J. Engineering for Industry, 1983, 105, pp. 31-38.

19. Otis, B. Y.H. Chee, J. Rabaey, "A 400microW Rx, 1.6mW Tx Super-regenerative transceiver for wireless sensor networks", IEEE ISSCC, 2005.

20. Hill, J., Culler, D., 2002. Mica: A Wireless Platform for Deeply Embedded Networks, *IEEE Micro*. Vol 22(6), Nov/Dec 2002, pp 12-24.

21.Dornfeld, D.A., "Design and Implementation of In-Process Sensors for the Control of Precision Manufacturing Processes," Advanced NDE Techniques (1998), pp. 125-150.